

## Electronic Supplementary Information (ESI) for

# Transition Metal Selenides as Efficient Counter Electrode Materials for Dye-sensitized Solar Cells

Jiahao Guo,<sup>‡ a,b</sup> Suxia Liang,<sup>‡ a</sup> Yantao Shi,<sup>a,\*</sup> Ce Hao,<sup>a</sup> Xuchun Wang,<sup>b</sup> and Tingli Ma<sup>c,d,\*</sup>

<sup>a</sup> State Key laboratory of Fine Chemicals, School of Chemistry, Dalian University of Technology, Dalian, 116024, P. R. China.  
E-mail: tinglima@dlut.edu.cn; shiyantao@dlut.edu.cn

<sup>b</sup> College of Chemistry and Materials Engineering, Anhui Science and Technology University, Fengyang, Anhui, 233100, P. R. China.

<sup>c</sup> School Petroleum and Chemical Engineering, Dalian University of Technology, Panjin Campus, Panjin 124221, P. R. China

<sup>d</sup> Graduate School of Life Science and Systems Engineering Kyushu Institute of Technology, Kitakyushu, Fukuoka, 808-0196, Japan

<sup>‡</sup> Jiahao Guo and Suxia Liang contributed equally to this work.

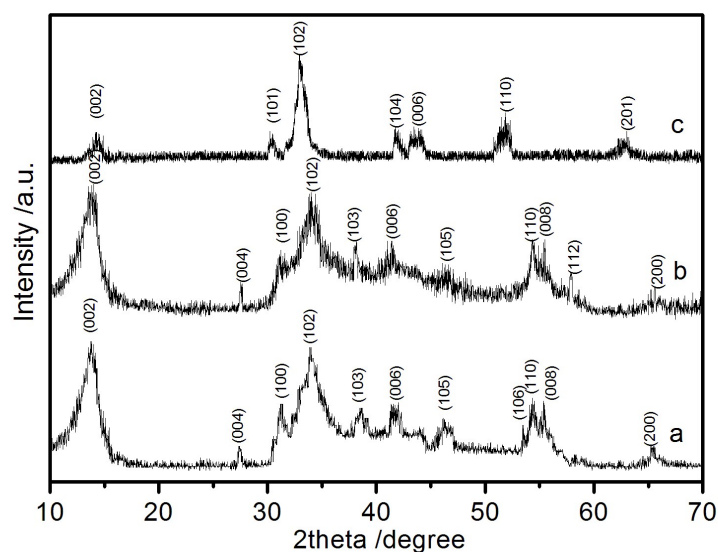


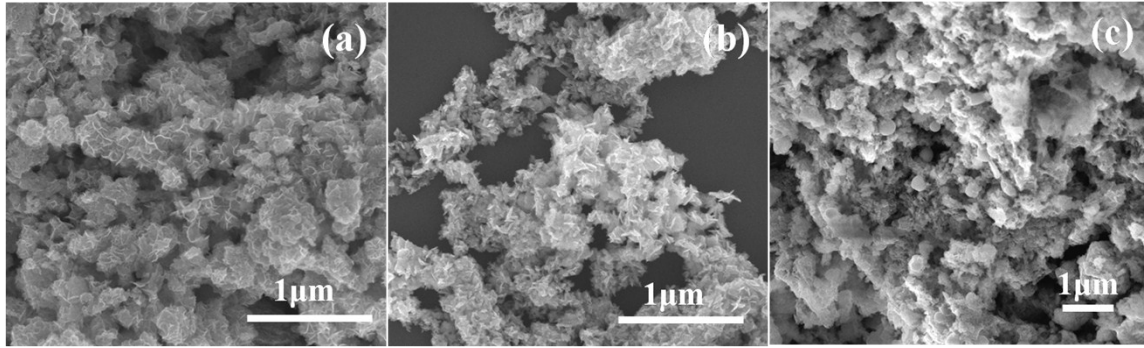
**Figure S1** XRD patterns of the synthesized three selenides. (a) MoSe<sub>2</sub>, (b) WSe<sub>2</sub>, and (c) TaSe<sub>2</sub>.

### X-ray diffractograms peak assignments of the synthesized five selenides

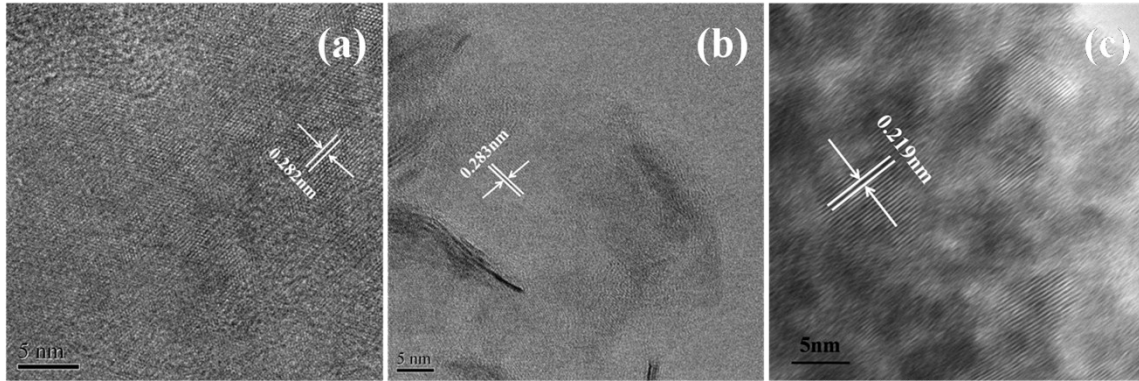
In Figure S1, for curve a, the diffraction peaks at 13.74°, 27.44°, 31.38°, 34.20°, 37.98°, 42.00°, 47.22°, 53.45°, 55.56°, 56.76°, and 65.30° are assigned to the crystal planes (002), (004), (100), (102), (103), (006), (105), (106), (110), (008), and (200), respectively (29-0914, PDF 2 database) and indicate that the hexagonal MoSe<sub>2</sub> was successfully synthesized. For WSe<sub>2</sub>, the diffraction peaks at 13.54°, 27.54°, 31.20°, 34.40°, 37.96°, 41.40°, 47.18°, 55.68°, 56.42°, 57.82°, and 65.58° are assigned to the crystal planes (002), (004), (100), (102), (103), (006), (105), (110), (008), (112) and (200), respectively (38-1388, PDF 2 database). For TaSe<sub>2</sub>, the diffraction peaks at 13.95°, 30.21°, 32.93°, 41.82°, 43.15°, 52.42°, and 62.77° are assigned to the crystal planes (002), (101), (102), (104), (006), (110), and (201), respectively (19-1303, PDF 2 database).

Table S1 Crystal structures, space groups, lattice parameters, and morphologies of the three TMSs.

Crystal structures	Space groups	Lattice parameters			Morphology
		a(Å)	b(Å)	c(Å)	
MoSe <sub>2</sub>	P63/mmc(194)	3.287	3.287	12.925	interlaced nanosheets
WSe <sub>2</sub>	P63/mmc(194)	3.286	3.286	12.983	nanoplates
TaSe <sub>2</sub>	P63/mmc(194)	3.436	3.436	12.696	fluffy nanoparticle



**Figure S2** Low-magnification SEM images of the three TMSs: (a) MoSe<sub>2</sub>, (b) WSe<sub>2</sub>, and (c) TaSe<sub>2</sub>.



**Figure S3** High resolution TEM images of (a) MoSe<sub>2</sub>, (b) WSe<sub>2</sub>, and (c) TaSe<sub>2</sub>. The high resolution TEM image of MoSe<sub>2</sub>, WSe<sub>2</sub>, and TaSe<sub>2</sub> (Figure S3b, c, and d) shows lattice fringes with spacing of 0.282 nm, 0.283nm, and 0.291nm, corresponding to the (100), (100), and (101) planes of hexagonal MoSe<sub>2</sub>, WSe<sub>2</sub>, and TaSe<sub>2</sub>, respectively.

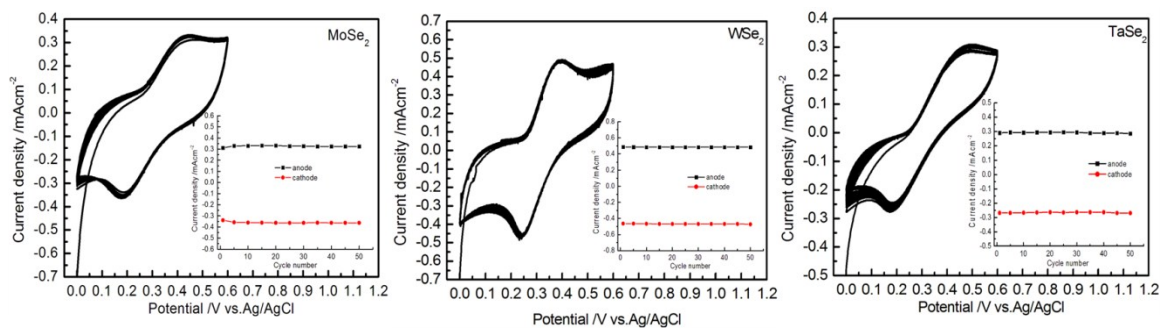


**Figure S4** 50 consecutive CVs of three TMS-based CE in electrolyte solution containing 2 mM LiI, 0.02 mM I<sub>2</sub>, and 20 mM LiClO<sub>4</sub>; the inset shows the anodic and cathodic peak current densities *versus* cycle time.

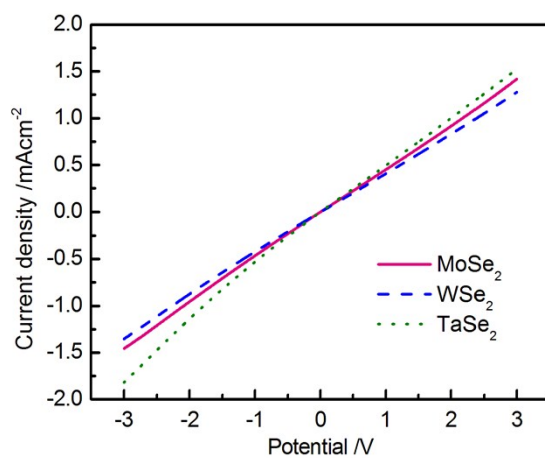


**Figure S5** *J-V* curves of CE/CE devices for different TMSs.

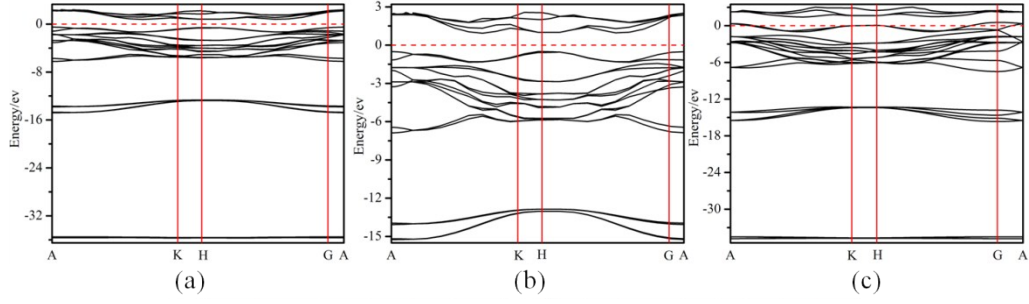


**Figure S6** Band structures of the three TMSs: (a) MoSe<sub>2</sub>, (b) WSe<sub>2</sub>, and (c) TaSe<sub>2</sub>.

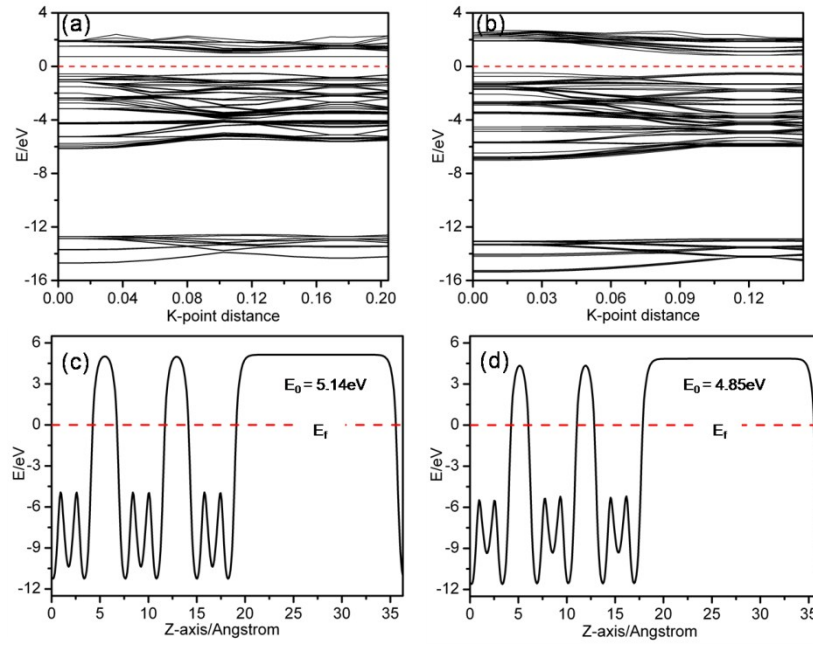


**Figure S7** The band structures of (c) MoSe<sub>2</sub> and (d) WSe<sub>2</sub> (001) surfaces and electrostatic potential along Z-axis for (a) MoSe<sub>2</sub> and (b) WSe<sub>2</sub> (001) surfaces.